

2011

Regional, extreme daily precipitation in NARCCAP simulations

Sho Kawazoe
Iowa State University

Follow this and additional works at: <https://lib.dr.iastate.edu/etd>

 Part of the [Earth Sciences Commons](#)

Recommended Citation

Kawazoe, Sho, "Regional, extreme daily precipitation in NARCCAP simulations" (2011). *Graduate Theses and Dissertations*. 10178.
<https://lib.dr.iastate.edu/etd/10178>

This Thesis is brought to you for free and open access by the Iowa State University Capstones, Theses and Dissertations at Iowa State University Digital Repository. It has been accepted for inclusion in Graduate Theses and Dissertations by an authorized administrator of Iowa State University Digital Repository. For more information, please contact digirep@iastate.edu.

Regional, extreme daily precipitation in NARCCAP simulations

by

Sho Kawazoe

A thesis submitted to the graduate faculty
in partial fulfillment of the requirements for the degree of

MASTER OF SCIENCE

Major: Meteorology

Program of Study Committee:

William J. Gutowski Jr., Major Professor
Eugene S. Takle
Raymond W. Arritt

Iowa State University

Ames, Iowa

2011

Copyright © Sho Kawazoe, 2011. All rights reserved.

Table of Contents

List of Tables.....	iii
List of Figures.....	iv
Abstract.....	v
Introduction.....	1
Chapter 1: Literature Review.....	3
1.1 Foundational Work.....	3
1.2 Extreme Precipitation.....	4
1.3 Extreme Precipitation Case Studies.....	7
Chapter 2: Observations, simulations, and analysis methods.....	9
2.1 Observations.....	9
2.2 Simulations.....	9
2.3 Analysis.....	11
Chapter 3: Widespread Extreme Precipitation.....	14
Chapter 4: Supporting Environmental Conditions.....	19
4.1 500hPa Geopotential Heights.....	19
4.2 10-m Horizontal Wind.....	20
4.3 2-m air temperature and specific humidity.....	21
Chapter 5: Conclusion.....	22
References.....	23
Acknowledgements.....	42

List of Tables

Table 1. Properties of NARCCAP models, CCSM, and UW: overall average precipitation rate and percentage of days reporting precipitation (parentheses: the percentage of days with 2.5-mm precipitation)	28
Table 2. Precipitation intensity for models and observations at the 95, 99, and 99.5th percentiles for all non-zero precipitation.....	29
Table 3. Percentage of widespread extremes occurring over two consecutive days and three consecutive days.....	30
Table 4. Percentage of extreme events by month for each model and observations. Highest values during the season are in bold. The RCM average is also shown.	31
Table 5. Percentage of extremes events by year of each model and observations. Highest values for each model are highlighted in bold. The RCM average is also shown.....	32

List of Figures

Figure 1. Region covered by each NARCCAP models, NARR, and CCSM. Analyzed region is highlighted: Upper Mississippi region.	33
Figure 2. Normalized frequency of precipitation as a function of daily intensity for 1982-1999 in all models and observation. Arrows mark the 99.5th percentile: red: CCSM, black:UW, blue: RCMs.	34
Figure 3. Days with simultaneous extremes on “N” grid points for all models and observations.	35
Figure 4. Composite daily precipitation during widespread extreme events: (a) UW, (b) CRCM, (c) ECP2, (d) HRM3, (e) MM5I, (f) RCM3, (g) WRFG, (h) GFDL, (i) CCSM. Contour scale for all plots is in the upper right, in mm day^{-1} . Region is highlighted by white box.	36
Figure 5. Composite 500-hPa during widespread extreme events: (a) NARR, (b) CRCM, (c) ECP2, (d) HRM3, (e) MM5I, (f) RCM3, (g) WRFG, (h) GFDL, (i) CCSM. Contour scale for all plots is in the upper right, in meters.	37
Figure 6. Composite 500-hPa anomalies during widespread extreme events: (a) NARR, (b) CRCM, (c) ECP2, (d) HRM3, (e) MM5I, (f) RCM3, (g) WRFG, (h) GFDL, (i) CCSM. Contour scale for all plots is in the upper right, in meters.	38
Figure 7. Composite 10-m horizontal winds during widespread extreme events: (a) NARR, (b) CRCM, (c) ECP2, (d) HRM3, (e) MM5I, (f) RCM3, (g) WRFG, (h) GFDL, (i) CCSM. CCSM wind data is archived at 09UTC, instead of 00 UTC used for other variables, accounting for the shift in location.	39
Figure 8. Composite 2-m temperature anomalies during widespread extreme events: (a) NARR, (b) CRCM, (c) ECP2, (d) HRM3, (e) MM5I, (f) RCM3, (g) WRFG, (h) GFDL, (i) CCSM. Contour scale for all plots is in the upper right, in Kelvin.	40
Figure 9. Composite 2-m specific humidity during widespread extreme events: (a) NARR, (b) CRCM, (c) ECP2, (d) HRM3, (e) MM5I, (f) RCM3, (g) WRFG, (h) GFDL, (i) CCSM. Contour scale for all plots is in the upper right, in kg kg^{-1} . CCSM specific humidity data is archived at 09UTC, instead of 00 UTC used for other variables, accounting for the shift in location.	41

Abstract

Extreme precipitation is a key topic in climate research. As the environment continues its steady increase in temperatures through increased greenhouse-gas emissions, conditions become more favorable for storm development that produce extreme events. This can have devastating effects in the upper Mississippi region, where agriculture dominates the regional economy.

To understand trends in extreme precipitation events of future climates, using climate models becomes essential. Because extreme precipitation events predominantly occur through relatively small-scale dynamics, the coarser resolution of global climate models (GCMs) is unable to capture fully such events. Therefore, regional climate models (RCMs) with higher resolution are used to simulate and investigate these events. In order to gain confidence in the models' ability to simulate future extreme events, we compare model simulations of contemporary climate with observations to determine if simulated extremes are occurring in conditions similar to the observed.

The overall objective of this work is to evaluate model performances from contemporary simulations by RCMs participating in the North American Regional Climate Change Assessment Program (NARCCAP). For comparison, we also examine output from a time-slice GCM of comparable resolution and a coarser atmosphere-ocean GCM. This work focuses on the upper Mississippi region for the winter season (December-January-February), when it is assumed that resolved synoptic circulation governs precipitation, comparing 18 years of simulations with observations.

For most of the models, average precipitation rates and percentage of days with precipitation is higher in models than observations. The high-resolution models generally reproduce well the precipitation-vs.-intensity spectrum seen in observations, with a small tendency toward producing overly strong precipitation at high intensity thresholds. Further analysis focuses on precipitation events exceeding the 99.5th percentile that occur simultaneously at 15 or more grid points in the region, yielding so-called “widespread events”. Collectively, the high-resolution models also tend to produce somewhat more frequent widespread events than the observations. Models capture the inter-seasonal variability well, as December in the observations and nearly all models are the month with the highest frequency of widespread extremes. Models produce fewer consecutive widespread-extreme days compared to observations. The atmosphere-ocean GCM has lower values of extreme precipitation frequency and intensity, likely because of its coarser resolution.

Further analysis focuses on 500 hPa flow, 10-m winds, 2-m temperatures, and 2-m specific humidity. The main feature yielding widespread extreme precipitation is an environment that is more favorable for the transport of moisture from the Gulf of Mexico into the analysis domain, and positive temperature and specific humidity anomalies, allowing the atmosphere to provide more moisture for precipitation.

Introduction

Very heavy and extreme precipitation events can cause costly and sometimes catastrophic floods in regions that may not be adequately prepared to combat such events. Although the causes of these events may vary, such as the Midwest floods of 1993 (e.g., Kunkel et al. 1994) and 2008 (e.g, Coleman and Budikova 2010), there is no question that these events cause immense social and economic stress to those that are affected. Furthermore, extreme events tend to be formed by a number of different conditions occurring simultaneously, which can act independently from each other, causing unpredictability in these events. Therefore, adequate simulations by models are vital, a need which has prompted substantial interest in the science community. In order to gain confidence in climate models' ability to simulate the environment when these extreme precipitation events are occurring, simulations need to be compared to observational data (Gutowski et al. 2010). By using projections, based on validated models, decisions and analysis with regard to future climate change can be made with much higher confidence.

Here we provide analysis of extreme daily precipitation events. Part of this paper is a continuation of work done by Gutowski et al. (2008), which focused on extreme winter precipitation in the upper Mississippi region, and its potential impacts under enhanced global warming scenarios. We use more models for our analysis through climate simulation produced by seven climate models for the North American Regional Climate Change Assessment Program (NARCCAP) (Mearns et al. 2009). The overall goal for this study is to assess the ability of the NARCCAP models collectively to reproduce extreme daily precipitation in observations, produce extreme precipitation for the same physical

conditions as in observations, and to provide a baseline for understanding how extreme daily precipitation and its causal processes change under enhanced greenhouse warming scenarios.

Although the study of extreme events has increased recently, few have looked into overall extreme precipitation during the winter in the upper Mississippi region. This may be due to winters in this region producing the least amount of precipitation when compared to other seasons (e.g., Dirmeyer and Kinter 2010), or lower frequency of extreme events compared to the rest of the year (Schumacher and Johnson 2006). However, winters on average have precipitation – evaporation (P-E) greater than zero (e.g., Seneviratne et al. 2004), and as a result, produce a net accumulation of surface and subsurface water (Gutowski et al. 2010). While winters generally produce less precipitation, heavy rainfall on frozen ground, with or without snow, can cause substantial flash flooding, as the surface is unable to absorb and hold moisture as effectively as in the warmer seasons (Huff and Angel 1992). Also, increased soil moisture during the winter will intensify the effect of extreme precipitation during the spring and summer, causing potentially severe hydrologic problems (Bell and Janowiak 1995).

This paper is arranged as follows. Chapter 1 reviews relevant literature. Chapter 2 gives description of models and observations, as well as the analysis that is used for this experiment. Analysis of extreme precipitation appears in Chapter 3, where we present further focus on what we term widespread events. We analyze the supporting conditions for these events in Chapter 4. The last chapter gives conclusions.

Chapter 1: Literature Review

1.1 Foundational Work

This thesis uses three papers as a basis for its study. The first paper, by Gutowski et al. (2007), looked at several regions in the US, including the upper Mississippi River basin, to compare simulated cold-season precipitation (October-March) with observations. In the upper Mississippi River basin, simulated average daily precipitation amounts were greater than observations. Model simulations also showed higher percentage of precipitation days, including events exceeding 2.5mm day^{-1} , although percentages were closer to observations at this threshold. Normalized frequency-versus-intensity plots showed models producing fewer precipitation events at higher values, indicating the models have difficulty simulating higher precipitation amounts.

The second paper (Gutowski et al. 2008) looked at widespread daily extreme precipitation in the upper Mississippi basin during the cold-season, again comparing simulations with observations. Similar to the first paper reviewed, model simulations showed greater average precipitation, but lower amounts of precipitation during extremes compared to observations. This study also looked at 500 hPa height fields for the day before, day of, and a day after widespread extremes. In the 500 hPa analysis, a cutoff low or deep trough occurred over the central US, and it was typically slow moving or stationary. This feature provided the upper Mississippi basin enhanced moisture from the Gulf of Mexico.

The third paper used as a basis for this thesis used the North American Regional Climate Change Assessment Program (NARCCAP) regional climate models (RCMs) to

analyze monthly extreme precipitation events during the cold-season (Gutowski et al. 2010). Unlike the previous two papers reviewed, which used one or two climate models with observations, this study used 6 RCMs from the NARCCAP project, comparing them with observational data. Overall, models showed good agreement with observations, as the spread among them was relatively small. For the upper Mississippi River basin, the models also captured the seasonal variation in the frequency of extreme events seen in observations, showing the highest occurrences during the cold season in November and March, and lowest occurrences of extreme precipitation in January and February. Models had some difficulty in simulating the higher extreme precipitation amounts, which was also seen in Gutowski et al. (2007). This work also considered the 500 hPa flow. The results are also consistent with Gutowski et al. (2008), where lower height anomalies occurred in the western half of the US, and higher height anomalies in the east, with the western anomalies likely caused by a deepening or cutoff low. The same pattern in the 500 hPa heights was seen in the monthly analysis.

1.2 Extreme Precipitation

Previous work that included extreme precipitation in the upper Mississippi region has tended to focus on the warmer half of the season, where higher rainfall intensity occurs. This is highlighted by studies such as Dirmeyer and Kinter (2010), who looked at the regional water cycle during floods over the U.S. Midwest. There, precipitation during the winter months (December-January-February) between 1979 and 2007 showed the lowest amount of mean precipitation compared to other seasons. Schumacher and Johnson (2006) showed that most extreme rain events during the summer season in the entire eastern half of

the U.S. are caused by Mesoscale Convective Systems, but nearly all cool-season events are associated with synoptic events. They also noted that summer extremes are more intense than in the winter, as temperatures are too cold for the atmosphere to contain and transport the necessary amounts of moisture into the upper Mississippi region.

Karl and Knight (1998) studied the frequency, amount, and intensity of precipitation events throughout the United States, especially at higher percentiles. Their work utilized station data, while filling in missing data using a gamma distribution (especially for earlier station data). They showed that increases of total precipitation are strongly affected by increases in both frequency and intensity of heavy and extreme precipitation, especially above the 90th percentile, relative to light and moderate precipitation. However, they saw insignificant changes in total winter precipitation in the upper Mississippi region during their time period of analysis (1910-1996).

Groisman et al. (2005) looked at trends in intense precipitation in climatic records for several regions of the globe. Their work had two sections, one of which used observational data from the National Climatic Data Center (NCDC) and the other of which used GCM output. Throughout the paper, the authors reminded the reader about the difficulty of using observational data due to the lack of readily available data outside of the contiguous United States, and the inhomogeneity of observational stations. Focusing on the region in his work of highest relevance to this thesis, the central United States has shown an increase in very heavy precipitation of about 20% from 1893 – 2002, with the largest increase in the last third of the twentieth century. The smaller amount of data from the early years of has added some noise to his analysis; nonetheless this increase is a relatively new phenomenon. The second portion of this paper used two GCMs that simulated climate

change from increasing CO₂ over the twenty-first century. Although direct comparison of GCMs to observations with respect to heavy precipitation is not commonly studied due to resolution issues and observational data variability (discussed earlier), simple detection analysis using model data showed that heavy precipitation is easier to detect and attribute to global warming compared to annual/seasonal mean precipitation. Warming temperatures also allow higher water content in the atmosphere, which can contribute to the increase. In addition, increased temperatures support an environment that is more favorable for convective storm development, which could help increase extreme precipitation events.

Other work by Groisman considered heavy precipitation, and its impacts on streamflow (Groisman et al. 2001). This paper also mentioned the shortcomings listed in Groisman et al. (2005), such as the inhomogeneity of station data, and whether or not these stations in the early years of the 1900s actually sampled adequately the extremes, since they are usually short lived and localized. The paper highlighted increasing trends of extreme precipitation in the upper Mississippi region. With temperature increases of about 0.5 °C since the start of the 1900s, extreme precipitation events might be expected to increase in frequency and intensity. Theoretically, heavy precipitation events should directly affect high streamflow events. When comparing days with precipitation and streamflow exceeding the 90th percentile of daily total precipitation and mean daily streamflow in the upper Mississippi region, Groisman et al. (2001) found fairly good correlation: 0.48. At higher percentiles, correlation values drop, likely because extreme precipitation is highly localized and thus not well-associated with river flow. Note also that a significant portion of extreme streamflow is related to snow melt, and earlier snowmelt in the last 50 years can alter precipitation versus streamflow correlations.

Bell et al. (2004) studied the ability of models to simulate extreme climatic events. Although this paper focused on California, and away from our analysis region, it does highlight some key points when using models. Regional climate models offer higher spatial resolutions compared to global climate models, allowing simulation and analysis of smaller-scale features. However, RCMs require lateral boundary conditions from global climate models, so global climate models are extremely important in producing good regional climate model simulations. Similar to work by Groisman et al. (2000, 2005), the lack of observational data prior to the industrial revolution undermines distinguishing between climate variability and climate change. However, Bell et al. (2004) note that climate models are our only tools for simulating future climates, despite their shortcomings. Finally, Bell et al. (2004) contend that a simple statement that warmer climates yield a stronger hydrologic cycle and a wetter world is misleading, because such a broad statement does not recognize that precipitation is highly variable regionally and temporally.

1.3 Extreme Precipitation Case Studies

Other papers that looked at extreme precipitation events have focused on case studies. A study done by Wendland et al. (1983) reviewed an unusually warm and moist winter of 1982-83. Although this paper did not study extreme precipitation exclusively, it did highlight some key aspects in its development. One important contributor to the higher than average precipitation during this particular winter was likely the abnormally high temperatures, which not only allowed the atmosphere to contain more moisture, but also caused a greater than average percentage of precipitation to fall in liquid form. Another case study by Bell and Janowiak (1995) looked at the atmospheric circulations during the

Midwest floods of 1993. Although this was not a study of extreme precipitation events during the winter months, it demonstrated the effect of above normal rainfall during the winter and spring years preceding the summer of 1993, which yielded high soil-moisture levels and thus helped exacerbate the flooding situation. It also showed the importance of a strong and persistent transport of moisture into the flood region from the Gulf of Mexico.

Chapter 2: Observations, simulations, and analysis methods

2.1 Observations

The analysis uses the University of Washington's (UW) gridded precipitation (Maurer et al. 2002) as its primary observational data. The dataset uses the Parameter-Elevation Regressions on Independent Slopes Model (PRISM; Daly et al. 1994) corrections for systematic elevation effects on precipitation climatology and provides observation-based precipitation on a 0.125° grid that covers all of the contiguous United States. Interpolation of gridded dataset by Maurer et al. (2002) used the scheme of Shepard (1984) as implemented in Widmann et al. (2000). This precipitation dataset in the NetCDF format covers the period 1950-1999.

We use the UW data output as the basis for identifying days when extreme precipitation occurs. For all other fields in the observational analysis, we use the North American Regional Reanalysis (NARR; Mesinger et al. 2006). The fields we use include 500hPa geopotential heights, 2-m air temperature, 2-m specific humidity and 10-m horizontal winds. These fields represent key environmental conditions during extreme precipitation development, and are also common to all models in NARCCAP, GCMs, and observations. Other potential fields of interest, such as moisture flux, are not common to all models.

2.2 Simulations

Model output comes from six regional climate models (RCMs) that simulated the period 1979-2003 for NARCCAP (Mearns et al. 2009): the Canadian Regional Climate

Model version 4 (designated CRCM in the NARCCAP archived), the Hadley Centre Regional Model version 3 (HadRM3; HRM3 in the archive), the NCAR Weather Research and Forecasting Model (WRF; WRFG in the archive), the fifth-generation Pennsylvania State University-NCAR Mesoscale Model (MM5; MM5I in the archive), the International Centre for Theoretical Physics Regional Climate Model version 3 (RegCM3; RCM3 in the archive), and the Experimental Climate Prediction Center's Regional Spectral Model (ECP2 in the archive). All models used approximately 0.5° resolution. Atmospheric boundary conditions, sea-surface temperatures (SSTs) and ocean ice fractions came from the reanalysis (Kanamitsu et al. 2002) produced by the National Center for Environmental Prediction (NCEP) and the U.S. Department of Energy (DOE). Except for the northern side, the boundaries in Figure 1 correspond roughly to the boundaries of each models' region that was interior to its outer frame where lateral boundary conditions were ingested. On the northern side, the interior region of the models extended into the northern Canadian territories. Further details of each model appear in both the NARCCAP web site (<http://narccap.ucar.edu>), and Mearns et al. (2009).

For comparison purposes, we also use output from two global climate models (GCMs): the Geophysical Fluid Dynamics Laboratory (GFDL) model, and the NCAR Community Climate System Model (CCSM). The GFDL model is a time-slice atmospheric GCM (AGCM) that simulated the period of 1968-1999 using GFDL's Atmospheric Model 2.1 (AM2.1). The simulation was part of the NARCCAP program and was run in Atmospheric Model Intercomparison Project (AMIP) mode at 0.5° resolution (GFDL Global Atmospheric Model Development Team 2004), like the NARCCAP RCMs. The model used observed SST sea-ice-extent from the Hadley Centre Sea Ice and Sea Surface

Temperature (HADISST) data set (Geophysical Fluid Dynamics Laboratory 2009). Use of the time-slice GCM helps to suggest differences in downscaling outcomes between a time-slice GCM and NARCCAP RCMs. The CCSM is an atmosphere-ocean GCM that supplied the boundary conditions to some later NARCCAP simulations of contemporary and future climate. Output from the CCSM is readily available in the same archive as the GFDL and NARCCAP RCMs. CCSM used T85 spectral resolution, roughly 1.4° grid spacing. We use the CCSM to compare the behavior of a relatively coarse resolution model versus the higher resolution RCMs and time-slice AGCM.

2.3 Analyses

We analyze the period 1982-99, discarding the years 1979-1981 for model spin up, and retaining years available in both observational and climate model data. We are working with extremes, so we adopt a relatively conservative spin-up period to ensure that the models water cycles are adequately spun up. Our region of interest is the upper Mississippi region, defined here as the region bounded by 37° - 47° N, 89° - 99° W, highlighted in Figure 1. This is the same definition used in previous analyses (Gutowski et al. 2007, 2008, 2010). Our analysis focuses on the winter season (December – February), when synoptic dynamics are more important than in the warmer months, when smaller scale convective events may be more important. This assumption here is that these events will be governed more by the resolved circulation (e.g., Schumacher and Johnson 2005, 2006, Gutowski et al. 2008)

In NARCCAP, the adopted “day” is 6UTC – 6UTC (midnight to midnight in the upper Mississippi region). The UW observational data set is already in daily increments in accordance to NARCCAP adopted day. The CCSM uses instantaneous data at 00 UTC,

because the model is stored as daily data. For all other models, we accumulated daily precipitation rate in accordance to the NARCCAP day. The original UW grid was converted to 0.5° by averaging all original grid points that fell in a 0.5° box centered on the new grid point. We did this to give the data set the same nominal resolution as the RCMs and time-slice GCM.

Analysis examining conditions other than precipitation during extreme events focuses on instantaneous data at 18UTC (local noon in the upper Mississippi region), which provides information on the state of the atmosphere during the day of an extreme event. Wind and temperature variables for CCSM are archived at 09UTC, which accounts for shifts in environmental trends.

We define a “precipitation event” as nonzero precipitation record for one day at one observational or model grid point, consistent with Gutowski et al. (2007). We extract events exceeding the top 0.5% of all precipitation events as extreme daily events. From these events, we then find widespread extremes by searching for multiple extremes events occurring on the same day. For our analysis, we designate simultaneous extremes on 15 or more grid points as widespread events. We select this threshold in order to have sufficient numbers of events to analyze while requiring enough spatial distribution that resolved synoptic dynamics could be governing factor. We examine several atmospheric fields, listed earlier, to understand conditions conducive to extremes. These fields give insight into the preferred conditions for extreme precipitation events and become the basis for assessing simulated versus observed processes yielding extreme precipitation. The 10-m winds were used as our primary indicator of moisture flux, although it is not synonymous with moisture flux direction and convergence. For some of the fields, we examine anomalies. These

anomalies are composites of fields on the days of widespread extreme events minus the 18-year time average during the winter season. Time averages are computed separately for each model and observations.

Chapter 3: Widespread Extreme Precipitation

Table 1 shows the overall average precipitation rate and frequency of all precipitation events in the upper Mississippi region. The numbers in parentheses are the percentage of days with precipitation above 2.5 mm day^{-1} , which is roughly 0.1inch, the reporting resolution of most U.S. rain gauges (Young et al. 1999). Other than WRFG, the models produce too much precipitation, with the GFDL and ECP2 models producing the most. Other than MM5I and WRFG, the models also produce too many days with precipitation, primarily due to too much light precipitation, or “drizzle”. This is evident by the number of precipitation days above 2.5 mm, for which the models tend to show closer agreement with the observations.

Figure 2 shows a histogram of normalized frequency vs. intensity in the upper Mississippi region. Intensity is separated into 2.5 mm day^{-1} bins. Models and observations show relatively good agreement up to about 30 mm day^{-1} . At higher intensities, observations are around the middle of the results. Except for the CCSM and CRCM, the models all have more days of intense precipitation than seen in the observations. The CCSM result may be a consequence of this model’s coarser resolution. The CRCM, on the other hand, agrees well with observations over the whole intensity spectrum. One should remember, however, that the University of Washington data set is gridded precipitation and the gridding process may smooth extremes. In the interpolation by Maurer et al. (2002), the radius of influence ranged from 50-100km, so the effective resolution of the dataset should be similar to the resolution of the RCMs. These results are not consistent with similar work by Gutowski et al. (2007), who diagnosed daily precipitation frequency versus intensity for

the same region. However, their study used two older RCMs and the cold half of the year (October-March). Those models did not produce precipitation as intense as observed. Part of the difference may be that the previous work used station data for observations. A comparison of Figure 2 here with Figure 2 of Gutowski et al. (2007) suggests that the gridding process to produce the University of Washington data set tends to smooth high intensity events.

Table 2 shows precipitation percentiles for each model and for the observations. The models and observations show fairly good agreement in terms of precipitation magnitude. The spread of precipitation amounts are also in good agreement, as the average of all models' 95th, 99th and 99.5th percentile is 9%, 15%, and 13% greater than observations, respectively. Excluding CCSM and/or GFDL does not change the spread significantly. Our previous studies looking at regional model performance in this region (e.g., Gutowski et al. 2003, 2007, 2008) focused on comparing one or two models to observations. These papers showed the models producing lower extreme precipitation than observations. But as Table 2 shows, especially for higher percentiles, the model extremes are mostly greater than observations. The CCSM is a coarser resolution model. It consistently has the lowest precipitation for each of the percentiles analyzed, suggesting that this models' coarser resolution does not allow it to replicate intense, small-scale circulation features that are vital for producing extremes.

Figure 3 shows the distribution of days with simultaneous extreme events on a given number of grid points. The x-axis indicates the area of a widespread event, suggesting its spatial scale. A grid point in the CCSM covers more area, so we adjusted the CCSM results to the equivalent number of half-degree grid boxes covered by one CCSM grid box by

multiplying the x-coordinate for CCSM results by $(1.4/0.5)^2 = 7.8$. The models tend to produce extreme events covering a wider area than the observations. In addition, CRCM and ECP2 have the largest spatial scales among the RCMs for their extreme events, which is noteworthy because these models also used interior nudging in which the models' wind fields are damped toward large-scale wind fields of the driving reanalysis. An implication of the figure is that the interior nudging produces extreme daily precipitation events that have larger spatial scale than observations or models not using the nudging.

Further analysis focuses on extremes occurring on at least 15 grid points on the same day. We denote these as widespread extreme events. As discussed above, we assume that the widespread events are especially likely to be the outcome of resolved behavior in the models.

Table 3 shows the normalized percentage of extremes on two or three consecutive days. The observational data show the highest percentage of two-and three-day extreme events. This may indicate that storms in these models either move out of the domain faster or decrease in strength more rapidly during their lifespan compared to observations. The MM5I and WRFG produce very low frequencies of consecutive extremes compared to the rest of the models and observations. This may be because their spatial scale (Figure 3) is smaller than other models or observations, so a relatively small location change could move the extreme out of the domain of interest.

Table 4 shows the distribution of extreme daily precipitation by winter months. Aside from RCM3, the models and observations show the most extremes occurring in December. This may be due to the warmer SST in the Gulf of Mexico during December compared to January and February. Warmer SST promotes warmer atmospheric

temperatures over the Gulf and thus promotes more atmospheric moisture for transport into the upper Mississippi region (e.g., Kunkel et al. 2002; Gutowski et al. 2008, 2010).

Table 5 shows interannual variability of extreme events for the models and observations as a percentage of all extremes from each data source. The “year” is the year for January and February. The average among all RCMs for each year also appears, for comparison purposes. Looking at the RCM average and the observations, the winters of 1983 and 1993 have larger numbers of extreme events than other years. The GFDL model also captures the higher extreme precipitation frequency of 1993. A case study done by Wendland et al. (1983) showed an unusually moist winter of the upper Midwest during 1983, when Iowa, for example, experienced the second wettest winter in 110 years. The 1993 Midwest floods were preceded by above average precipitation during the preceding winter and spring months, which saturated the soil, exacerbating the flooding by above average summer precipitation (Bell and Janowiak 1995). We also calculated correlations between pairs of RCM, GCM, and UW time series. The resulting correlations, 0.287 for RCM/GFDL, -0.018 for GFDL/UW, and 0.452 for RCM/UW, show that the RCM average matches observations better than the time-slice model. Although these results use only one time-slice model, they suggest that the RCMs replicate the observed interannual variability of extremes when using reanalysis boundary conditions because of their lateral boundary conditions.

Figure 4 shows composite precipitation during widespread extremes. Models and observations show similar locations of extremes, centered near the southern boundary of our analysis region. Our analysis region in winter is warmest to the south. The warmer air can contain more precipitable water, so the composite extreme precipitation occurs where

there will generally be more moisture in the atmosphere. Also, the southern end of the analysis region is closest to the primary source of the region's precipitable water, the Gulf of Mexico. This analysis is consistent with Liang et al. (2004), who also showed the observed average winter precipitation gradient decreasing from the southeast to northwest within our analysis region.

Chapter 4: Supporting Environmental Conditions

Figures 5 – 9 show composite fields produced by averaging over the widespread event days from each data source. Again, the anomaly fields for a given source come from subtracting the 18-year DJF average from the composite. The NARR provides the observational results, with the days to composite determined from analysis of the UW precipitation.

4.1 500 hPa Geopotential Heights

As suggested by Figure 5, a key ingredient for extreme precipitation in the upper Mississippi region is the transport of warm, moist air from the Gulf of Mexico. Composite 500 hPa heights and composite height anomalies for each model (Figure 6) show the extreme events occurring when a deep trough develops around the southern Rockies, promoting a more pronounced southerly flow into the region when compared with seasonal climatology. Anomaly plots also show areas of higher heights in the northeast, suggesting that the occurrences of both low heights to the west and high heights to the east are important in extreme precipitation development. Inspection of the individual events shows that the composites are representative of the behavior in each case, except that in some individual cases, the deep trough includes a cut-off low center at 500 hPa. In height plots, the day before and the day after extreme events 500 hPa height patterns have a slow or stationary propagation of the trough, with roughly the same speed of movement in the observations and the models.

4.2 10-m Horizontal Wind

Figure 7 shows the composite 10-m winds for widespread extreme events. As with 500 hPa heights, the composites are representative of the behavior of individual events. As discussed earlier, the winds indicate the direction of moisture transport and also the location of surface pressure centers. Again, these winds are not synonymous with the moisture flux direction and convergence, also discussed earlier.

During the widespread extreme events, winds decrease and turn counter-clockwise behind the area of extreme precipitation. The behavior corresponds to a surface low in the vicinity of Oklahoma accompanying the 500 hPa trough. Composite precipitation moves as the low center moves (not shown). Wedland et al. (1983), who focused on higher than average precipitation during the 1982-83 winter, also had a surface low in the vicinity of Oklahoma during strong precipitation. In addition, the behavior shows low-level convergence. Because relatively strong winds blow from the Gulf of Mexico, the momentum convergence likely coincides with the moisture convergence, especially in the vicinity of the extreme precipitation.

Winds in the Gulf of Mexico highlight the importance of surface high pressure to the east of the analysis region. Strong winds in the composites tend to start as southwesterly flow around the southern tip of Florida. Over the Gulf, the winds turn clockwise toward the northern coast. This pattern provides substantial fetch for moistening air before it enters the southern U.S. Moreover, this flow pattern passes over the Loop Current, where SST tends to be warmer due to a consistent flow of warmer Caribbean waters into the southern Gulf (Vukovich 2007). Flow over the Loop Current may supply additional moisture into the southern portion of our domain.

4.3 2-m air temperature and specific humidity

We also analyze 2-m air temperature and specific humidity from most of the models and the NARR. The CCSM is an exception, as 2-m specific humidity was not available from the NARCCAP archive. Instead, we used specific humidity at the model level closest to the surface (approx. 993 hPa), and assumed that its spatial characteristics are similar to 2-m values. Figures 8 and 9 show these two fields as composite anomalies. Regions of extreme precipitation tend to occur in regions of higher temperatures and specific humidity compared to climatology. Plots of temperature and specific humidity one day before and after the widespread extreme events (not shown) generally support an anomalously warmer and wetter environment during the development and propagation of these events. Also, composite temperature analysis in areas of extreme precipitation is above 275K, which increases the likelihood that the precipitation type during these events is liquid precipitation.

Chapter 5: Conclusion

Six different climate models and one time-slice GCM from the NARCCAP project, and one AOGCM were compared with observational data (NARR and UW) to determine the ability of models to reproduce extreme precipitation events during the winter months (December-February) between 1982-1999 in the upper Mississippi region. Widespread extreme precipitation is defined as the top 0.5% of all non-zero precipitation occurring on at least 15 grid points simultaneously. For these events, we analyzed 500hPa heights, 2-m air temperature and specific humidity, and 10-m surface winds to diagnose the environment that is favorable for the production of extreme precipitation.

Most models agree that extremes peak in December during the winter months, likely due to warmer SST in the Gulf of Mexico, allowing more transport of moisture into the central US. Models for the most part, tend to produce too much precipitation when compared to observations. Also, models tend to produce too many days with precipitation, with a large portion of it being in the form of light precipitation, or “drizzle”. CRCM and ECP2, which incorporated interior nudging, suggests that interior nudging increases the spatial scale of extreme precipitation events. For precipitation extremes at 95th, 99th, and 99.5th percentiles, the models are consistently near or above observations (except for the CCSM, which has coarser resolution). Models and observations are in good agreement for frequency vs. intensity of precipitation up to about 30 mm day⁻¹. Above this value, and except for two RCMs, the models also produce several days with precipitation amounts that are higher than any in the observations.

For environmental features, the observations and models show similar characteristics. Composite 500hPa heights show a predominant southwesterly flow into the upper Mississippi region, caused by a deep trough or cutoff low around the Rockies. This allows increased moisture transport into the central United States from the Gulf of Mexico, which aids the development of extreme precipitation. Anomaly plots show areas experiencing maximum extreme precipitation tend to occur in areas of positive anomalies of surface air temperatures, which provide an environment capable of holding more moisture compared to climatology. Areas experiencing maximum extreme precipitation also tend to occur in areas of positive moisture anomalies, showing that the warmer air does indeed yield greater moisture. Surface wind analysis suggests a strong transport of Gulf of Mexico moisture into the upper Mississippi region. Features of a surface low exist slightly to the west of the area of extreme precipitation. Low-level momentum convergence of 10-m winds near extremes is also present, indicating possible moisture convergence. Extremes tend to occur near the southern portion of the analysis region, centered on central Missouri. This is likely due to the warmer air in the southern part of the analysis region and transport of Gulf of Mexico moisture into the domain.

References

- Bell, G.D., and J. E. Janowiak, 1995: Atmospheric Circulation Associated with the Midwest Floods of 1993. *Bull. Amer. Meteor. Soc.*, **76**, 681-695.
- Bell, J.L., L.C. Sloan, and M.A. Snyder, 2004: Regional Changes in Extreme Climatic Events: A Future Climate Scenario. *J. Climate*, **17**, 81-87.

- Coleman, J.S.M., and D. Budikova, 2010: Atmospheric aspects of the 2008 Midwest floods: a repeat of 1993? *International Journal of Climatology*, **30**, 1645-1667.
- Daly, C., R.P. Neilson, and D.L. Phillips, 1994: A statistical-topographic model for mapping climatological precipitation over mountainous terrain. *J. Appl. Meteor.*, **33**, 140-158.
- Dirmeyer, P.A., and J.L. Kinter, 2010: Floods over the U.S. Midwest: A Regional Water Cycle Perspective. *J. Hydrometeor.*, **11**, 1172-1181.
- Geophysical Fluid Dynamics Laboratory, 2009: Time slice experiments at approximately 50km resolution. [Available online at [http:// www.gfdl.noaa.gov/narccap-am2--data](http://www.gfdl.noaa.gov/narccap-am2--data)]
- GFDL Global Atmospheric Model Development Team, 2004: The new GFDL global atmosphere and land model AM2/LM2: Evaluation with prescribed SST simulations. *J. Climate*, **17**, 4641-4673.
- Groisman, P.Y., R.W. Knight, and T.R. Karl. 2001: Heavy Precipitation and High Streamflow in the Contiguous United States: Trends in the Twentieth Century. *Bull. Amer. Meteor. Soc.*, **82**, 219-246.
- , R.W. Knight, D.R. Easterling, T.R. Karl, G.C. Hegerl, and V.N. Razuvaev, 2005: Trends in Intense Precipitation in the Climatic Record. *J. Climate*, **18**, 1326-1350.
- Gutowski, W.J., S.G. Decker, R.A. Donavon, Z. Pan, R.W. Arritt, and E.S. Takle, 2003: Temporal–Spatial Scales of Observed and Simulated Precipitation in Central U.S. Climate. *J. Climate*, **16**, 3841-3847.

- , E.S. Takle, K.A. Kozak, J.C. Patton, R.W. Arritt, and J.H. Christensen, 2007: A Possible Constraint on Regional Precipitation Intensity Changes under Global Warming. *J. Hydrometeor.*, **8**, 1382-1396.
- , S.S. Willis., J. C. Patton, B.R.J. Schwedler, R.W. Arritt, and E.S. Takle, 2008: Changes in extreme, cold-season synoptic precipitation events under global warming. *Geophys. Res. Lett.*, **35**, L20710, doi:10.1029/2008GL035516.
- , R.W. Arritt, S. Kawazoe, D.M. Flory, E.S. Takle, S. Biner, D. Caya, R.G. Jones, R. Laprise, L.R. Leung, L.O. Mearns, W. Moufouma-Okia, A.M.B. Nunes, Y. Qian, J.O. Roads, L.C. Sloan, and M.A. Snyder, 2010: Regional Extreme Monthly Precipitation Simulated by NARCCAP RCMs. *J. Hydrometeor.*, **11(6)**, 1373-1379
- Huff, F.A., and J.R. Angel. 1992: Rainfall frequency atlas of the mid-west. Bull. 71. Illinois State Univ., Champaign, IL.
- Kanamitsu, M., W. Ebisuzaki, J. Woollen, S.K. Yang, J.J. Hnilo, M. Fiorino, and G.L. Potter, 2002: NCEP/DOE AMIP-II reanalysis (R-2). *Bull. Amer. Meteor. Soc.*, **83**, 1631-1643.
- Karl, T.R., and R.W. Knight, 1998: Secular Trends of Precipitation Amount, Frequency, and Intensity in the United States. *Bull. Amer. Meteor. Soc.*, **79**, 231-241.
- Kunkel, K.E., S.A. Changnon, and J.R. Angel, 1994: Climatic aspects of the 1993 Upper Mississippi River Basin flood. *Bull. Amer. Meteor. Soc.*, **75**, 811-822.
- , K. Andsager, X.-Z. Liang, R.W. Arritt, E.S. Takle, W.J. Gutowski, and Z. Pan, 2002: Observations and Regional Climate Model Simulations of Heavy

- Precipitation Events and Seasonal Anomalies: A Comparison. *J. Hydrometeor.*, **3**, 322-334.
- Liang, X.-Z., L. Li, K.E. Kunkel, M. Ting, and J.X.L. Wang, 2004: Regional Climate Model Simulation of U.S. Precipitation during 1982–2002. Part I: Annual Cycle. *J. Climate*, **17**, 3510-3529.
- Maurer, E.P., A.W. Wood, J.C. Adam, D.P. Lettenmaier, and B. Nijssen, 2002: A long-term hydrological based dataset of land surface fluxes and states for the conterminous United States. *J. Climate*, **15**, 3237-3251.
- Mearns, L. O., W. J. Gutowski, R. Jones, L.-Y. Leung, S. McGinnis, A. M. B. Nunes, and Y. Qian, 2009: A regional climate change assessment program for North America. *Eos, Trans. Amer. Geophys. Union*, **90**, 311-312.
- , et al., 2007, updated 2011: *The North American Regional Climate Change Assessment Program dataset*, National Center for Atmospheric Research Earth System Grid data portal, Boulder, CO. Data downloaded 2011-04-25.
[<http://www.earthsystemgrid.org/browse/viewProject.htm?projectId=ff3949c8-2008-45c8-8e27-5834f54be50f>]
- Mesinger, F., and Coauthors, 2006: North American Regional Reanalysis. *Bull. Amer. Meteor. Soc.*, **87**, 343-360.
- Schumacher, R.S., and R.H. Johnson, 2005: Organization and Environmental Properties of Extreme-Rain-Producing Mesoscale Convective Systems. *Mon. Wea. Rev.*, **133**, 961-976.
- , and R.H. Johnson, 2006: Characteristics of U.S. Extreme Rain Events during 1999–2003. *Wea. Forecasting*, **21**, 69-85.

- Seneviratne, S.I., P. Viterbo, D. Lüthi, and C. Schär, 2004: Inferring Changes in Terrestrial Water Storage Using ERA-40 Reanalysis Data: The Mississippi River Basin. *J. Climate*, **17**, 2039-2057.
- Shepard, D.S., 1984: Computer Mapping: The SYMAP interpolation algorithm. *Spatial Statistics and Models*, G.L. Gaile and C.J. Willmott, Eds., D. Reidel, 133-145.
- Vukovich, F.M., 2007: Climatology of Ocean Features in the Gulf of Mexico Using Satellite Remote Sensing Data. *J. Phys. Oceanogr.*, **37**, 689-707.
- Wendland, W.M., L.D. Bark, D.R. Clark, R.B. Curry, J.W. Enz, K.G. Hubbard, V. Jones, E.L. Kuehnast, W. Lytle, J. Newman, F.V. Nurnberger, and P. Waite, 1983: Review of the Unusual Winter of 1982-83 in the Upper Midwest. *Bull. Amer. Meteor. Soc.*, **64**, 1346-1356.
- Widmann, M., and C.S. Bretherton, 2000: Validation of Mesoscale Precipitation in the NCEP Reanalysis Using a New Gridcell Dataset for the Northwestern United States. *J. Climate*, **13**, 1936-1950.
- Young, C. B., B. R. Nelson, A. A. Bradley, J. A. Smith, C. D. Peters-Lidard, A. Kruger, and M. L. Baeck, 1999: An evaluation of NEXRAD precipitation estimates in complex terrain. *J. Geophys. Res.*, **104**, 19691-19703.

Source	Average Precipitation Rate (mm/day)	Days with Precipitation (%)
UW	1.09	55.4 (11.7)
CCSM	1.22	90.0 (12.0)
GFDL	1.75	87.0 (16.6)
CRCM	1.30	83.5 (13.0)
ECP2	1.67	67.6 (15.8)
HRM3	1.39	67.3 (11.8)
MM5I	1.23	51.0 (12.2)
RCM3	1.35	77.6 (13.7)
WRFG	0.98	41.9 (9.8)

Table 1. Properties of NARCCAP models, CCSM, and UW: overall average precipitation rate and percentage of days reporting precipitation (parentheses: the percentage of days with 2.5-mm precipitation)

Source	95% (mm/day)	99% (mm/day)	99.5% (mm/day)
UW	8.77	19.58	25.40
CCSM	6.18	15.24	19.52
GFDL	9.68	23.50	30.90
CRCM	6.76	18.15	24.30
ECP2	11.78	26.59	34.78
HRM3	10.92	27.24	35.06
MM5I	11.23	24.19	30.55
RCM3	8.29	20.00	25.11
WRFG	11.54	24.02	29.21

Table 2. Precipitation intensity for models and observations at the 95, 99, and 99.5th percentiles for all non-zero precipitation.

Source	Percent of Cons. Extremes (2 days)	Percent of Cons. Extremes (3 days)
UW	47.5%	22.5%
CCSM	25.0%	0.0%
GFDL	43.9%	5.3%
CRCM	32.8%	4.7%
ECP2	38.0%	6.0%
HRM3	40.4%	5.8%
MM5I	13.8%	0.0%
RCM3	38.0%	10.3%
WRFG	15.4%	0.0%

Table 3. Percentage of widespread extremes occurring over two consecutive days and three consecutive days.

Source	December	January	February
UW	50.0%	25.0%	25.0%
CCSM	45.8%	22.9%	31.3%
GFDL	40.4%	22.8%	36.8%
CRCM	42.2%	31.3%	26.6%
ECP2	44.0%	22.0%	34.0%
HRM3	46.2%	25.0%	28.8%
MM5I	44.8%	34.5%	20.7%
RCM3	30.0%	34.0%	36.0%
WRFG	46.2%	34.6%	19.2%
RCM	42.2%	30.2%	27.6%

Table 4. Percentage of extreme events by month for each model and observations. Highest values during the season are in bold. The RCM average is also shown.

Year	UW	CCSM	GFDL	CRCM	ECP2	HRM3	MM5I	RCM3	WRFG	RCM
1982	7.5%	6.3%	5.3%	3.1%	2.0%	5.8%	0.0%	2.0%	3.8%	2.8%
1983	12.5%	6.3%	7.0%	10.9%	8.0%	13.5%	13.8%	4.0%	7.7%	9.6%
1984	0.0%	10.4%	8.8%	1.6%	6.0%	3.8%	0.0%	4.0%	0.0%	2.6%
1985	10.0%	6.3%	3.5%	7.8%	6.0%	1.9%	6.9%	2.0%	7.7%	5.4%
1986	5.0%	6.3%	8.8%	3.1%	4.0%	1.9%	6.9%	0.0%	0.0%	2.7%
1987	2.5%	4.2%	7.0%	4.7%	2.0%	7.7%	0.0%	6.0%	7.7%	4.7%
1988	10.0%	0.0%	3.5%	3.1%	2.0%	5.8%	3.4%	4.0%	3.8%	3.7%
1989	2.5%	12.5%	1.8%	4.7%	2.0%	9.6%	6.9%	2.0%	3.8%	4.8%
1990	2.5%	4.2%	8.8%	4.7%	8.0%	7.7%	6.9%	2.0%	3.8%	5.5%
1991	5.0%	4.2%	3.5%	7.8%	6.0%	5.8%	10.3%	6.0%	11.5%	7.9%
1992	0.0%	0.0%	1.8%	7.8%	2.0%	5.8%	3.4%	8.0%	0.0%	4.5%
1993	12.5%	4.2%	10.5%	7.8%	10.0%	5.8%	10.3%	14.0%	15.4%	10.6%
1994	2.5%	4.2%	8.8%	3.1%	8.0%	1.9%	0.0%	10.0%	0.0%	3.8%
1995	5.0%	2.1%	0.0%	3.1%	6.0%	1.9%	0.0%	6.0%	7.7%	4.1%
1996	2.5%	6.3%	5.3%	4.7%	8.0%	0.0%	0.0%	4.0%	0.0%	2.8%
1997	7.5%	0.0%	5.3%	9.4%	6.0%	7.7%	6.9%	8.0%	7.7%	7.6%
1998	0.0%	4.2%	8.8%	3.1%	6.0%	5.8%	13.8%	6.0%	15.4%	8.3%
1999	7.5%	8.3%	1.8%	7.8%	4.0%	1.9%	10.3%	8.0%	3.8%	6.0%
2000	5.0%	10.4%	0.0%	1.6%	4.0%	5.8%	0.0%	4.0%	0.0%	2.6%

Table 5. Percentage of extremes events by year of each model and observations. Highest values for each model are highlighted in bold. The RCM average is also shown.

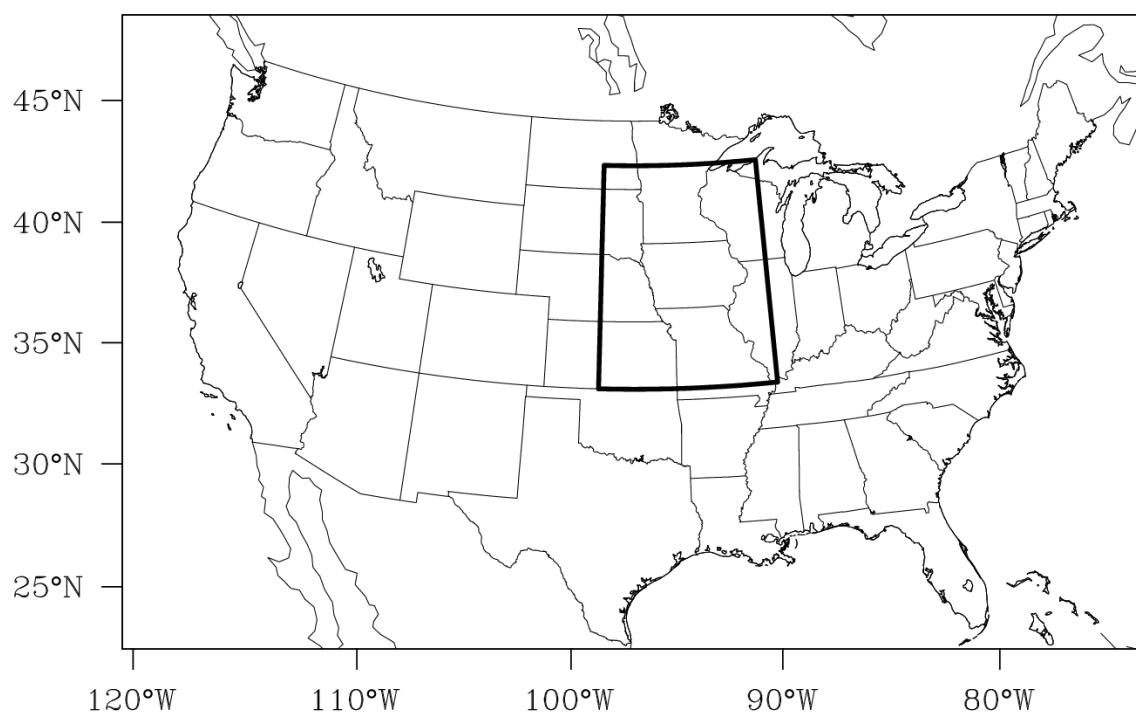


Figure 1. Region covered by each NARCCAP models, NARR, and CCSM. Analyzed region is highlighted: Upper Mississippi region.

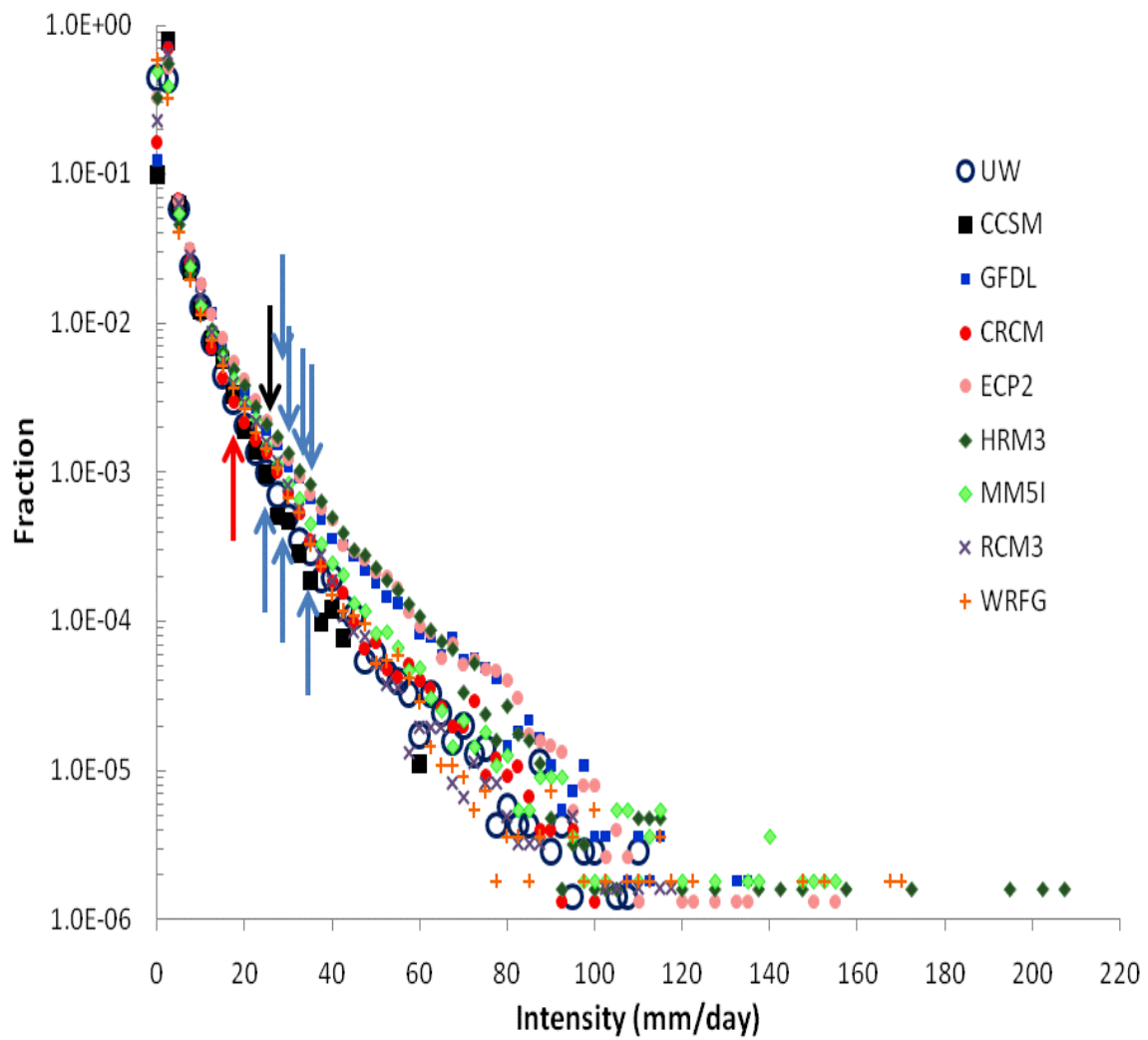


Figure 2. Normalized frequency of precipitation as a function of daily intensity for 1982-1999 in all models and observation. Arrows mark the 99.5th percentile: red:CCSM, black:UW, blue: RCMs.

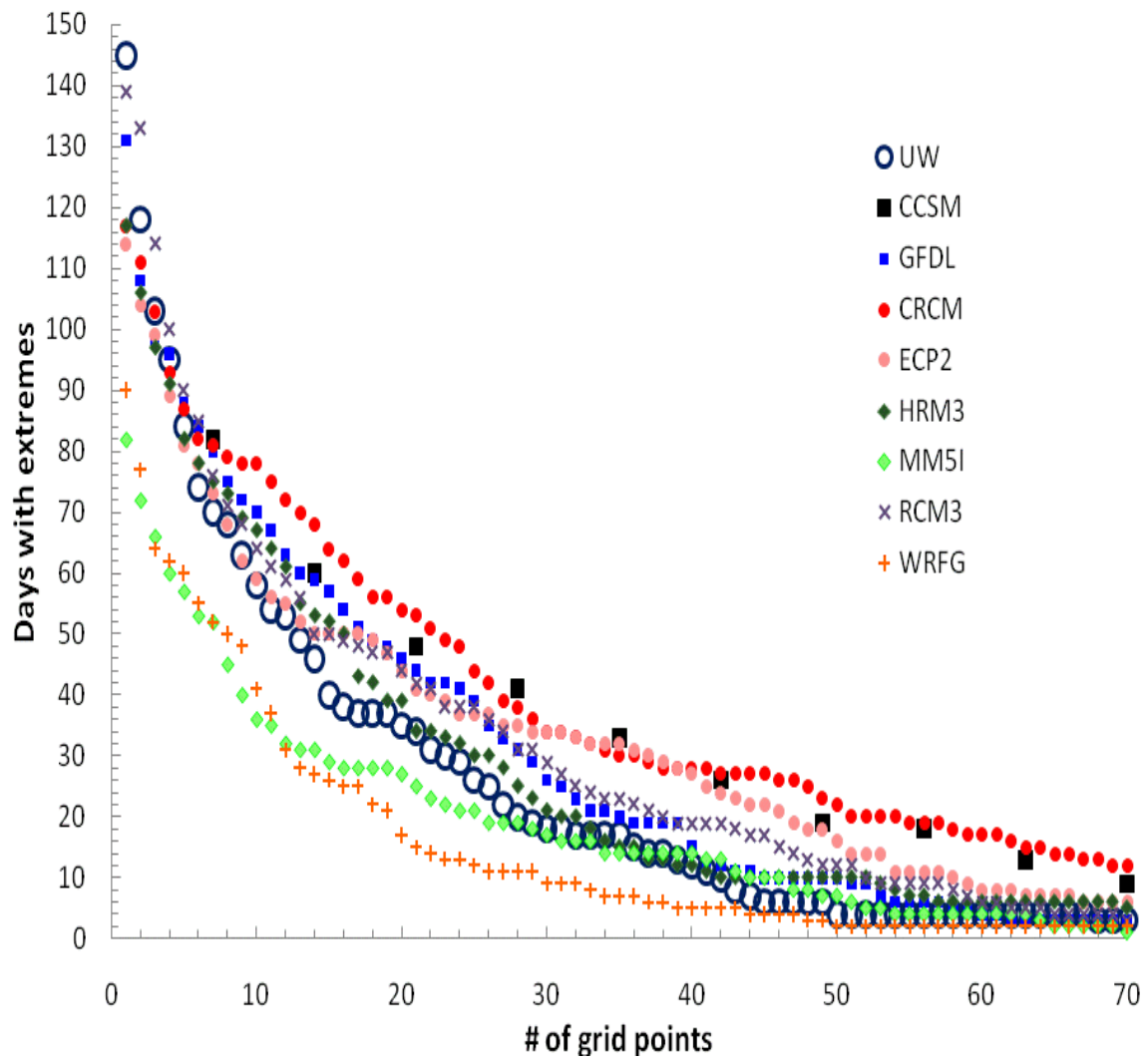


Figure 3. Days with simultaneous extremes on “N” grid points for all models and observations.

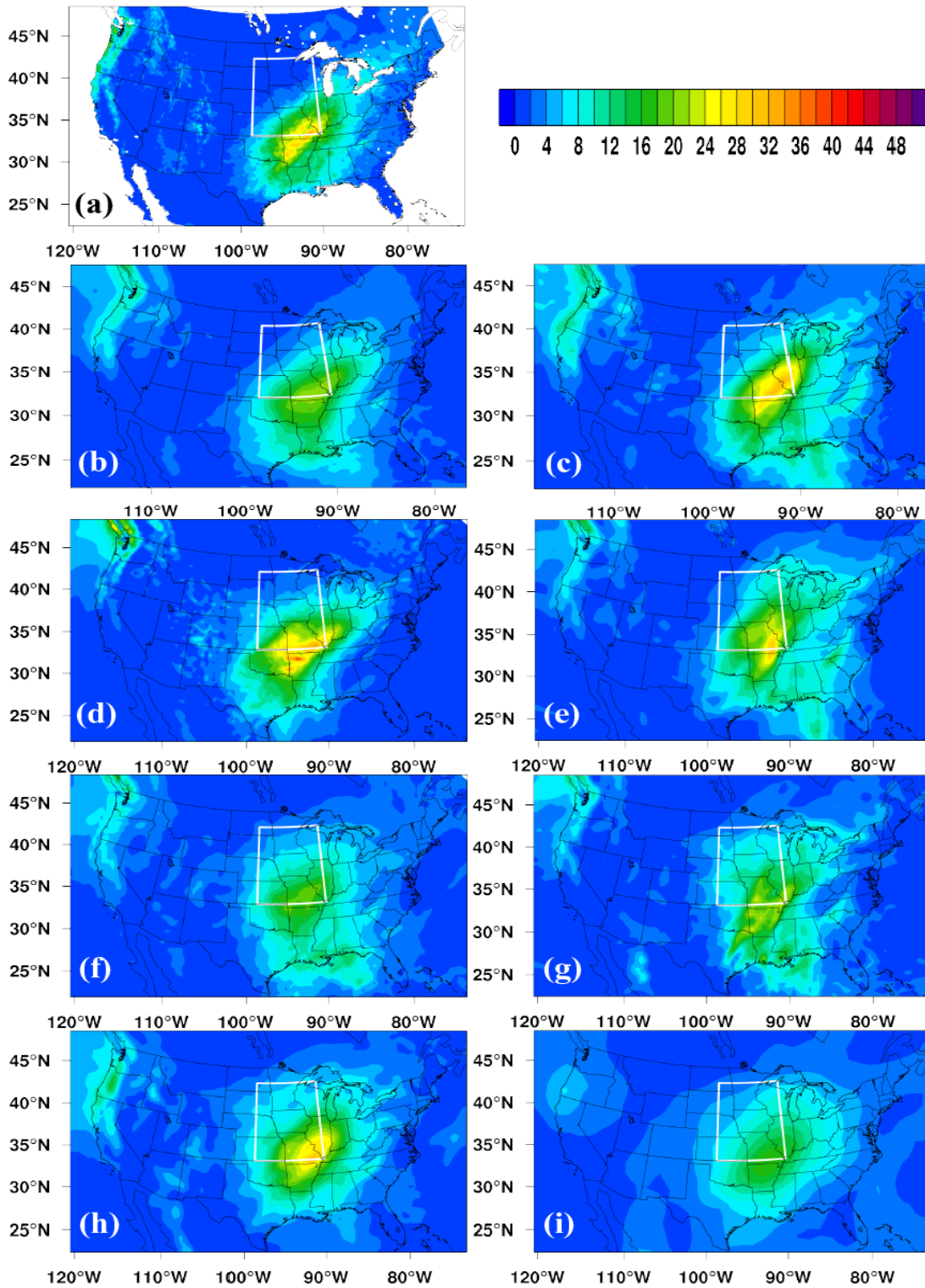


Figure 4. Composite daily precipitation during widespread extreme events: (a) UW, (b) CRCM, (c) ECP2, (d) HRM3, (e) MM5I, (f) RCM3, (g) WRFG, (h) GFDL, (i) CCSM. Contour scale for all plots is in the upper right, in mm day^{-1} . Region is highlighted by white box.

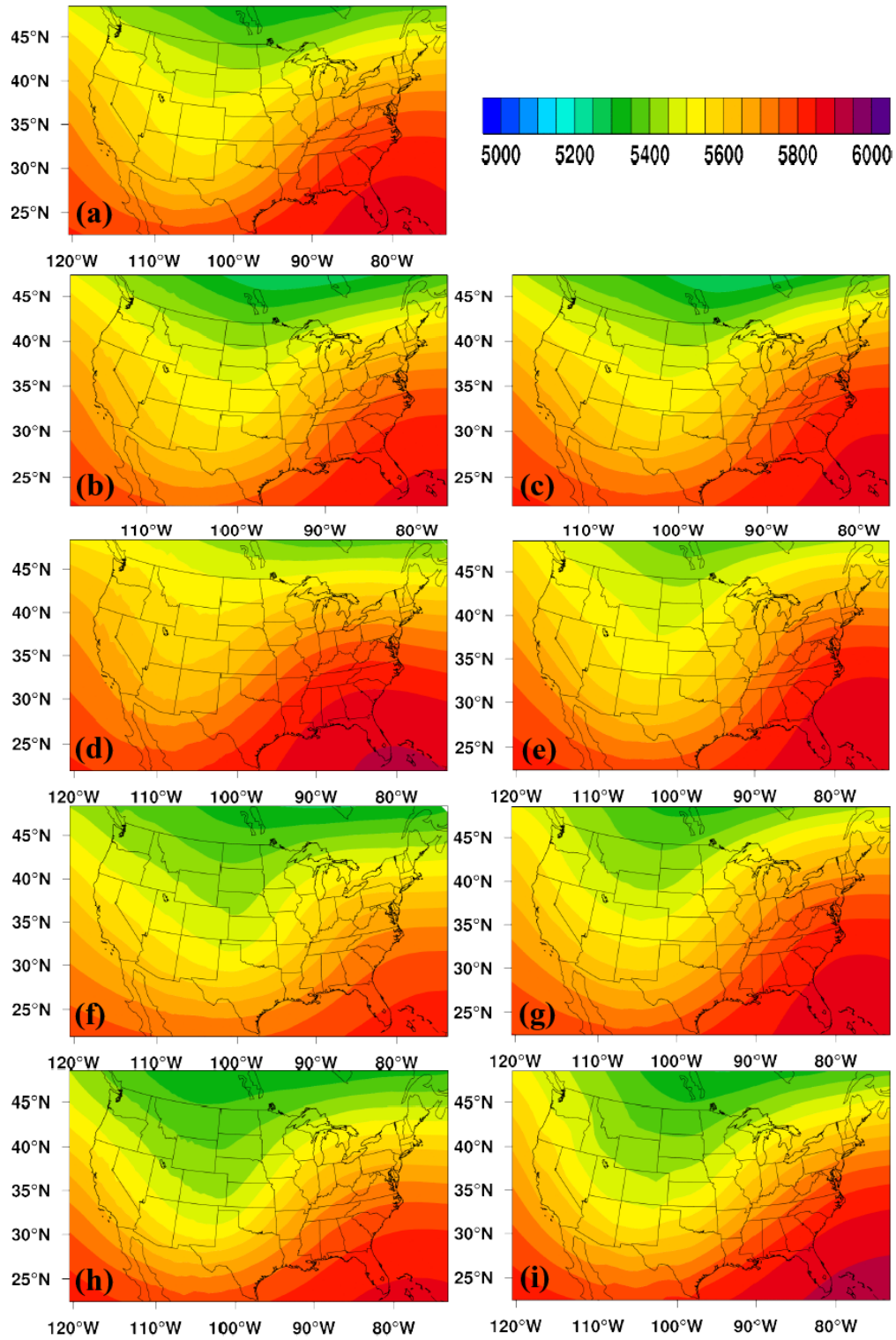


Figure 5. Composite 500-hPa during widespread extreme events: (a) NARR, (b) CRCM, (c) ECP2, (d) HRM3, (e) MM5I, (f) RCM3, (g) WRFG, (h) GFDL, (i) CCSM. Contour scale for all plots is in the upper right, in meters.

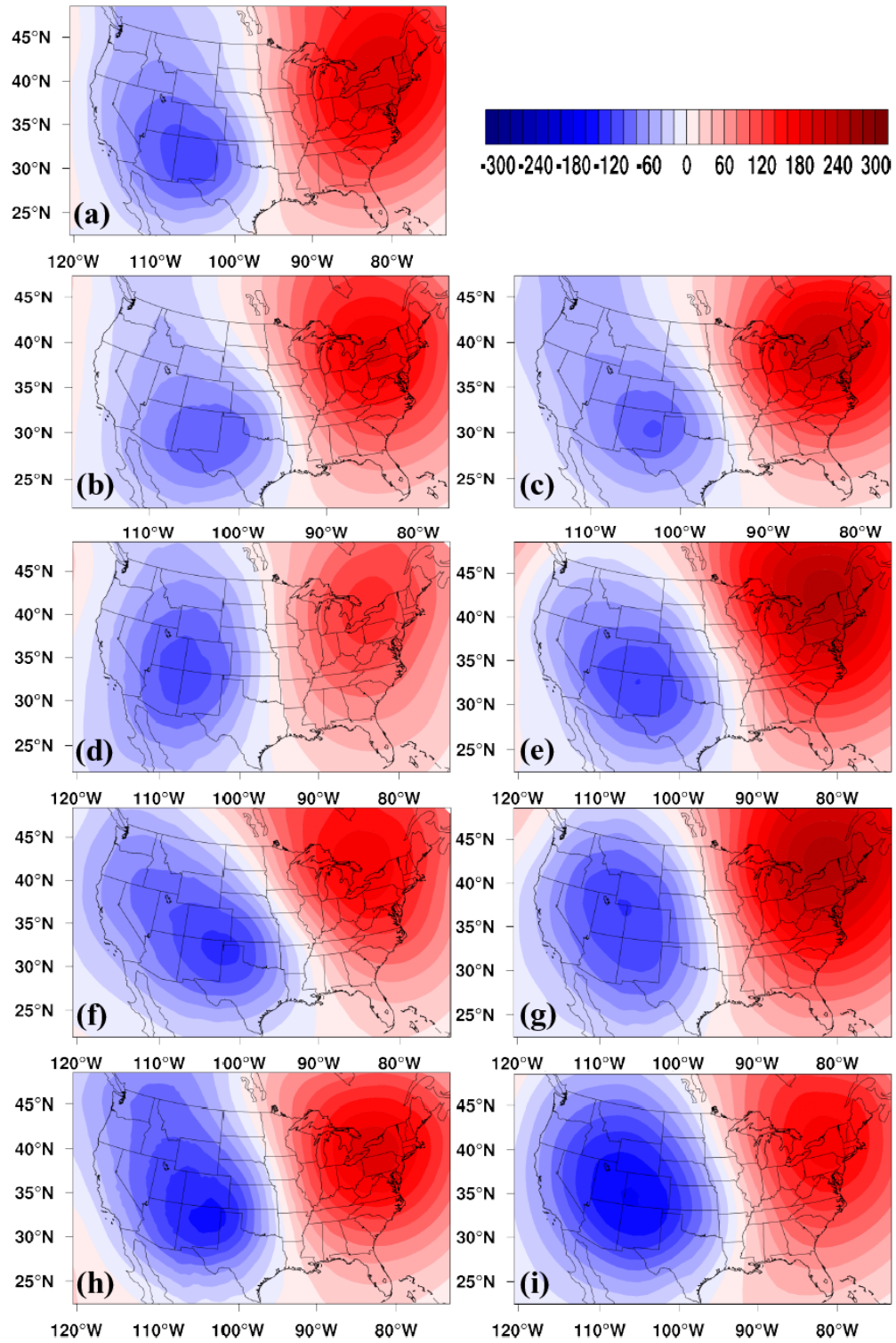


Figure 6. Composite 500-hPa anomalies during widespread extreme events: (a) NARR, (b) CRCM, (c) ECP2, (d) HRM3, (e) MM5I, (f) RCM3, (g) WRFG, (h) GFDL, (i) CCSM. Contour scale for all plots is in the upper right, in meters.

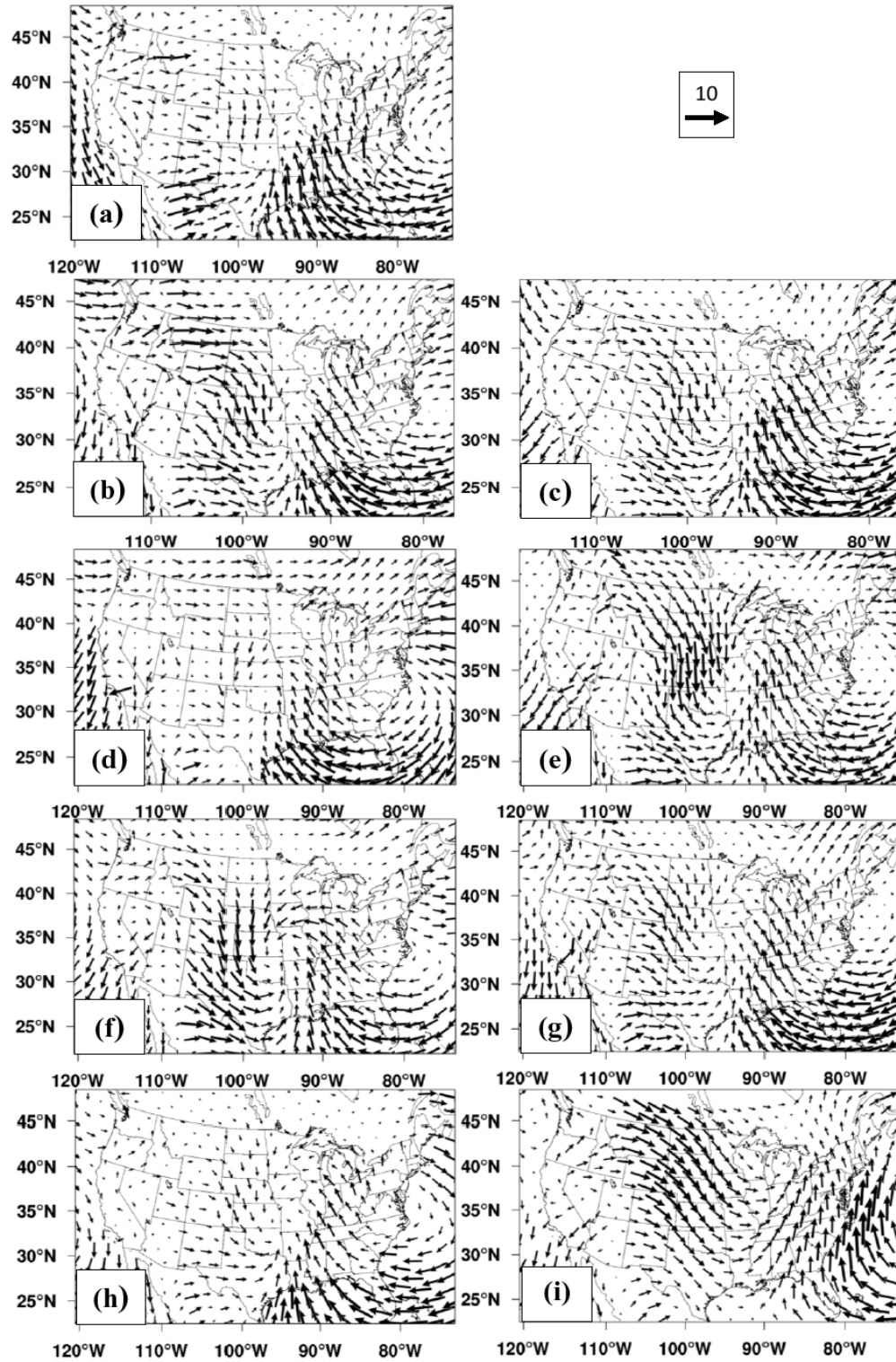


Figure 7. Composite 10-m horizontal winds during widespread extreme events: (a) NARR, (b) CRCM, (c) ECP2, (d) HRM3, (e) MM5I, (f) RCM3, (g) WRFG, (h) GFDL, (i) CCSM. CCSM wind data is archived at 09UTC, instead of 00 UTC used for other variables, accounting for the shift in location.

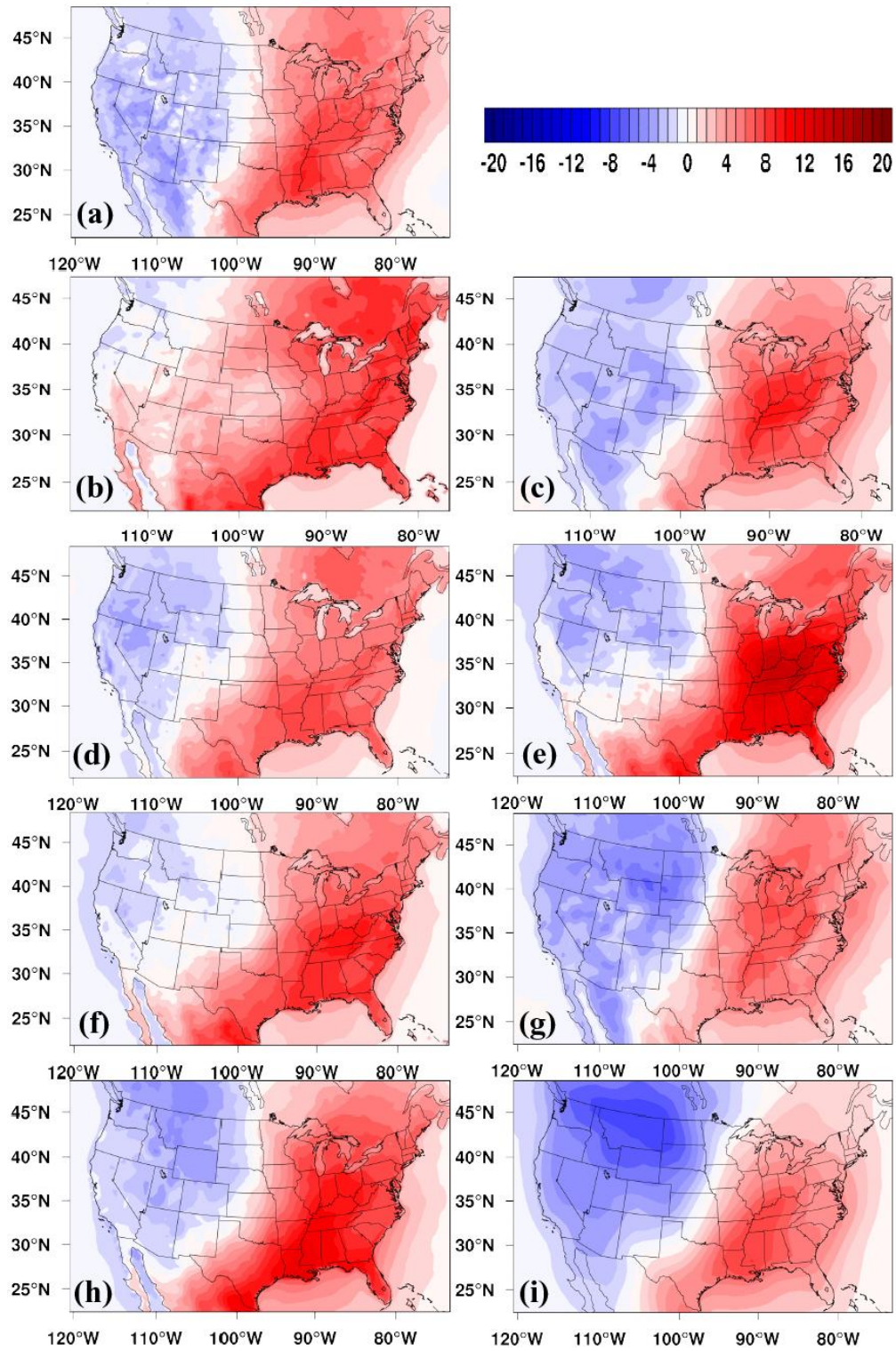


Figure 8. Composite 2-m temperature anomalies during widespread extreme events: (a) NARR, (b) CRCM, (c) ECP2, (d) HRM3, (e) MM5I, (f) RCM3, (g) WRFG, (h) GFDL, (i) CCSM. Contour scale for all plots is in the upper right, in Kelvin.

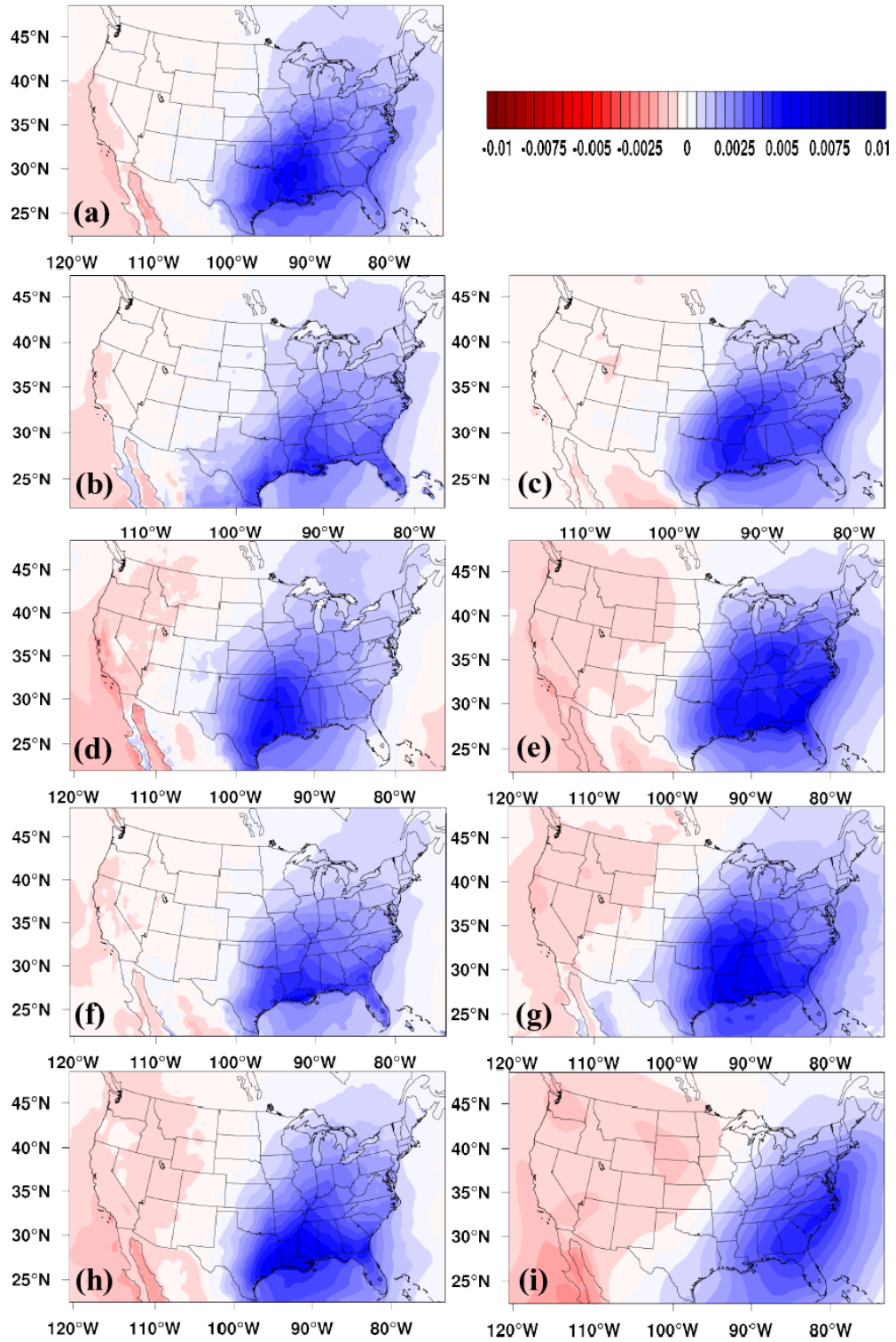


Figure 9. Composite 2-m specific humidity during widespread extreme events: (a) NARR, (b) CRCM, (c) ECP2, (d) HRM3, (e) MM5I, (f) RCM3, (g) WRF3, (h) GFDL, (i) CCSM. Contour scale for all plots is in the upper right, in kg kg^{-1} . CCSM specific humidity data is archived at 09UTC, instead of 00 UTC used for other variables, accounting for the shift in location.

Acknowledgements

First, I would like to thank my advisor, Dr. William Gutowski, for allowing me an opportunity to work under him in pursuit of not only my master's degree, but also for his assistance on my senior research project in my final year as an undergraduate. He was instrumental in introducing this topic to me, and has guided me every step of the way. I truly appreciate the dedication he was shown for me, and I have, and will continue to relish the opportunity to work under him.

I thank my office mates, Brandon Fisel and Justin Glisan. They were instrumental in my understanding of NCL, as well as being a helpful resource for any other questions I may have had. I thank Dave Flory, for his commitment to me during both my graduate and undergraduate career, to my friends and faculty for their support and encouragements, and to my family for their commitment to me, and allowing me the freedom and opportunity to chase after my dream far away from home.